Supporting Information for

Engineering Defective Trimetallic Metal-Organic Framework Nanosheets for Advanced Water Oxidation Electrocatalysis

Hui Xu [a, b], Cheng Wang [b], Guangyu He [a*], Haiqun Chen [a*]

[a] *Key Laboratory of Advanced Catalytic Materials and Technology, Advanced Catalysis and Green Manufacturing Collaborative Innovation Center, Changzhou University, Changzhou, Jiangsu Province 213164, China*

[b] *College of Chemistry Chemical Engineering and Materials Science, Soochow University, Suzhou, 215123 P. R. China*

Corresponding authors: hegy@cczu.edu.cn (G. He); chenhq@cczu.edu.cn (H. Chen)

Chemicals

Nickel(II) acetate tetrahydrate ($Ni(OAc)_2 \cdot 4H_2O$), iron(II) sulfate heptahydrate ($FeSO_4 \cdot 7H_2O$), cobalt(II) sulfate heptahydrate ($CoSO_4 \cdot 7H_2O$), manganese(II) sulfate monohydrate ($MnSO_4 \cdot H_2O$), zinc(II) sulfate heptahydrate ($ZnSO_4 \cdot 7H_2O$), cadmium(II) sulfate ($CdSO_4 \cdot 3H_2O$), terephthalic acid (1,4-H_2BDC), N,N-dimethylacetamide (DMAC) were purchased from Sinopharm Chemical Reagent Co. Ltd (Shanghai, China). Other chemicals and solvents were obtained from commercial suppliers and used without further purification.

Characterizations

The samples were examined by powder X-ray diffraction (PXRD), which was conducted on a X'Pert-Pro MPD diffractometer (Netherlands PANalytical) with a Cu Kα X-ray source (λ = 1.540598 Å). The morphology of the products was studied by

transmission electron microscopy (TEM, HITACHI HT7700) and scanning transmission electron microscopy (STEM, FEI Tecnai F20). Scanning electron microscopy (SEM) images and energy dispersive X-ray spectroscopy (EDS) were taken with a HITACHI S-4700 cold field-emission scanning electron microscope operated at 15 kV. X-ray photoelectron spectra (XPS) were collected with an SSI S-Probe XPS Spectrometer.

Electrochemical measurements

Electrochemical measurements were made using a three-electrode setup with a Hg/HgO electrode as the reference electrode and a graphite rod as the counter electrode, a glassy carbon (GC) disk electrode (5 mm in diameter) was used as the working electrode. The catalyst suspension was prepared by dispersing 5 mg catalyst containing 3.5 mg of MOF in 1 mL solution containing 0.97 mL isopropanol and 30 μL 0.5 wt. % Nafion solution followed by ultrasonication for 1 h. The above suspension (20 μL) was dropped on to the polished GC electrode and then dried at room temperature. The overpotential (η) was calculated according to the following formula: η= ERHE - 1.23 V. Linear sweep voltammetry (LSV) was recorded in an O_2-saturated 1.0 M KOH solution at a scan rate of 5 $mV \cdot s^{-1}$ and room temperature to obtain the polarization curves. The cyclic voltammetry for 60 cycles is also operated for activating the working electrode. The stability tests were performed by chronopotentiometry at the current density of 10 $mA \cdot cm^{-2}$. The electrochemical double-layer capacitance (C_{dl}) was determined from cyclic voltammograms measured in a non-Faradaic region at different scan rates (v = 10, 20, 30, and 40 mV/s) in the

potential range 1.1 to 1.2 V versus RHE. The current differences at 0.05 V against scan rates were fitted to obtain the C_{dl}: $C_{dl} = I_c/v$, where C_{dl}, I_c, and v are the double-layer capacitance (mF/cm^2) of the electroactive materials, charging current (mA/cm^2), and scan rate (mV/s). Electrochemical impedance spectra (EIS) experiments were performed with the three-electrode cell system in 1M KOH at 25°C. The amplitude of the sinusoidal wave was 10 mV, and the frequency scan range was from 10 kHz to 100 mHz

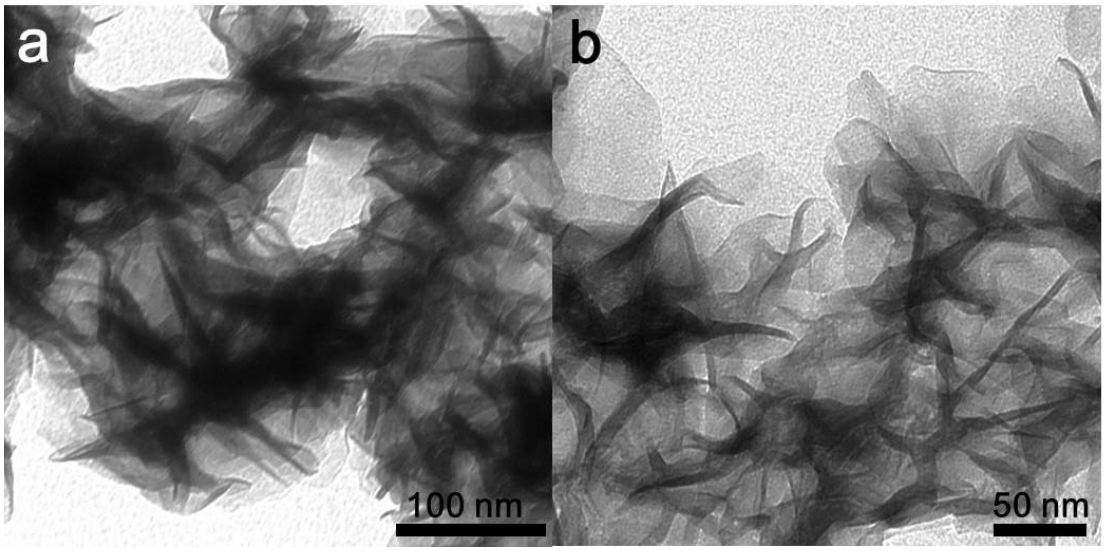

Fig.S1 Additional TEM images of the NiFeZn MOF nanosheets.

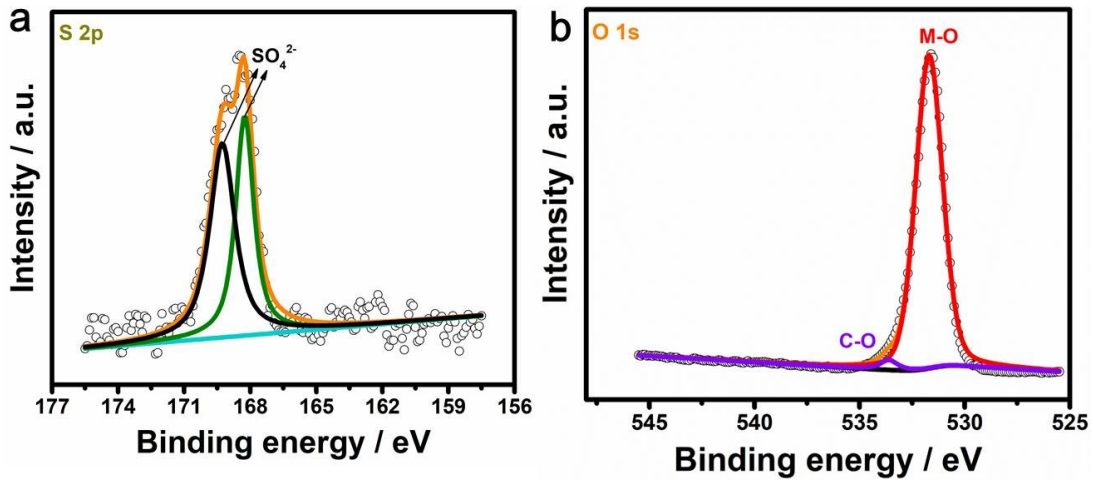

Fig.S2 High-resolution XPS spectra of the (a) 2p and (b) 1s.

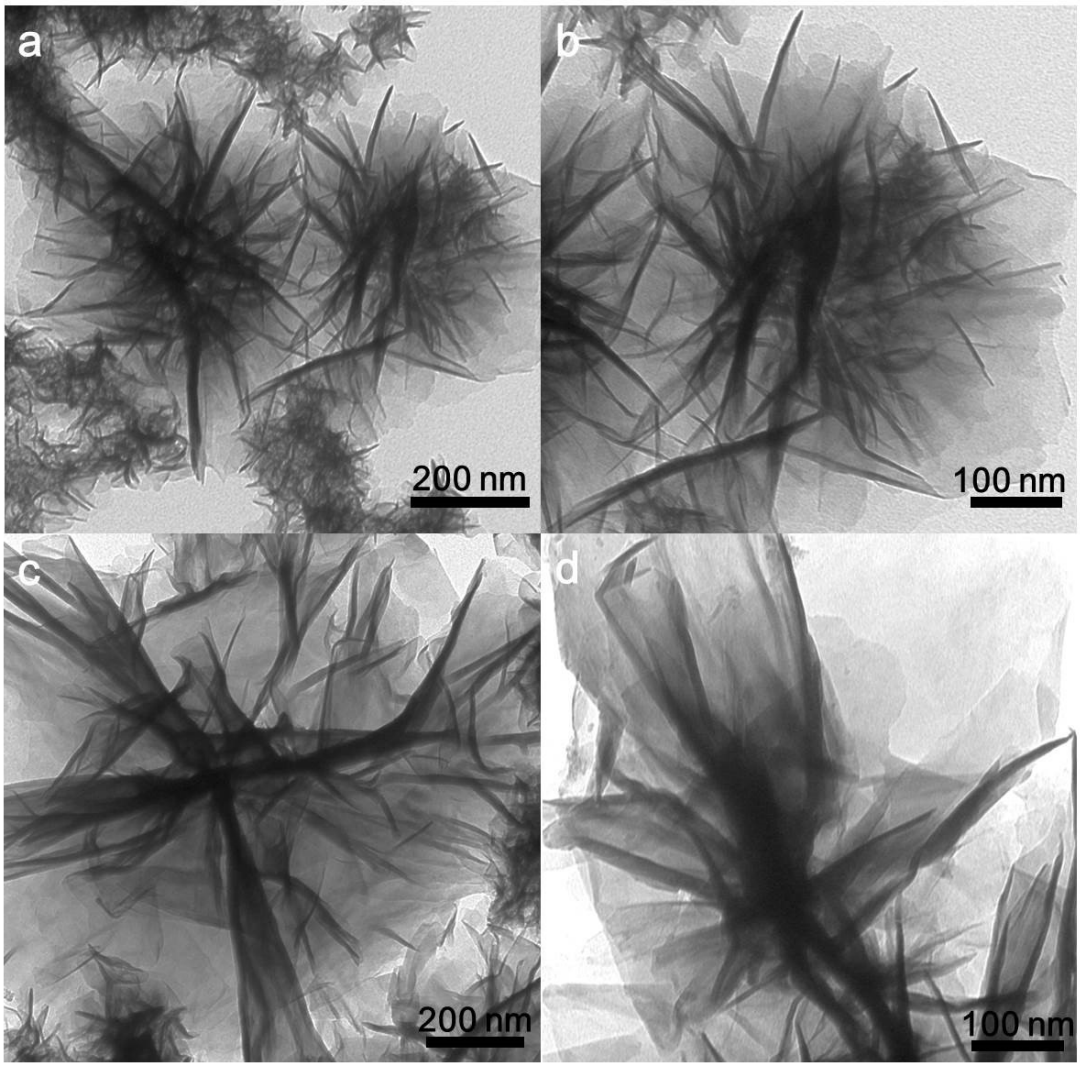

Fig.S3 Representative TEM images of the (a, b) NiFeZn-1 and (c, d) NiFeZn-5 MOF nanosheets.

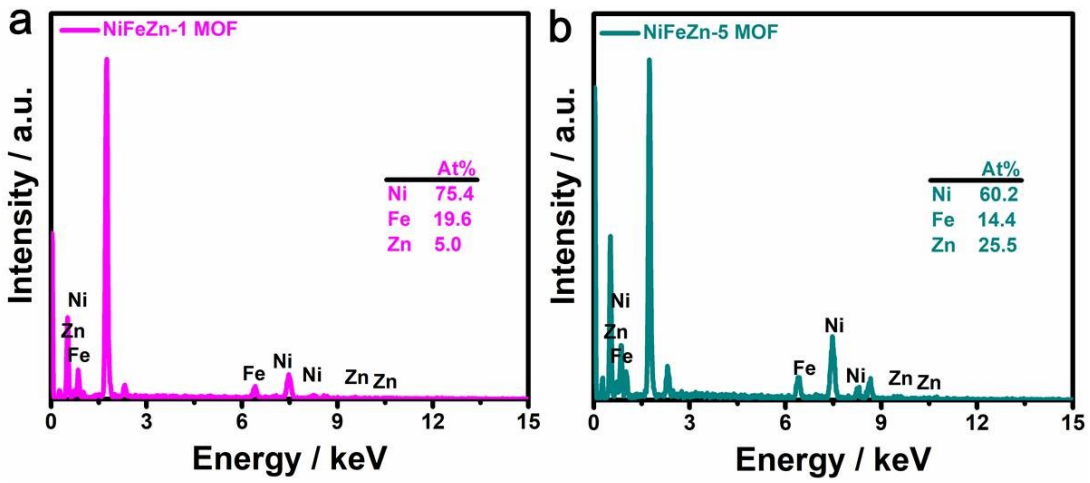

Fig.S4 SEM-EDX spectra of the (a) NiFeZn-1 and (b) NiFeZn-5 MOF nanosheets.

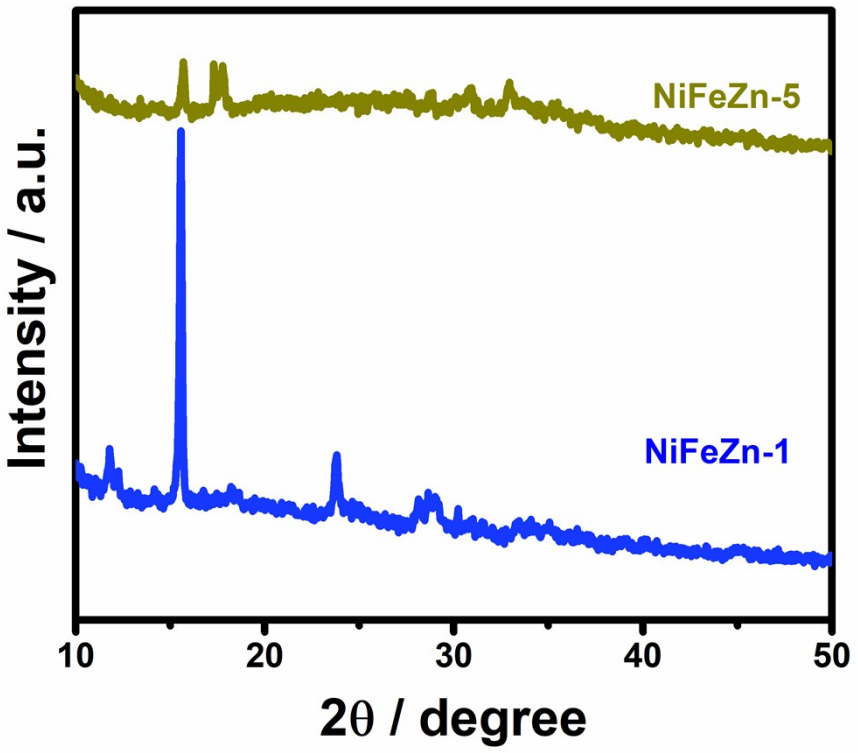

Fig.S5 XRD patterns of the (a) NiFeZn-1 and (b) NiFeZn-5 MOF nanosheets.

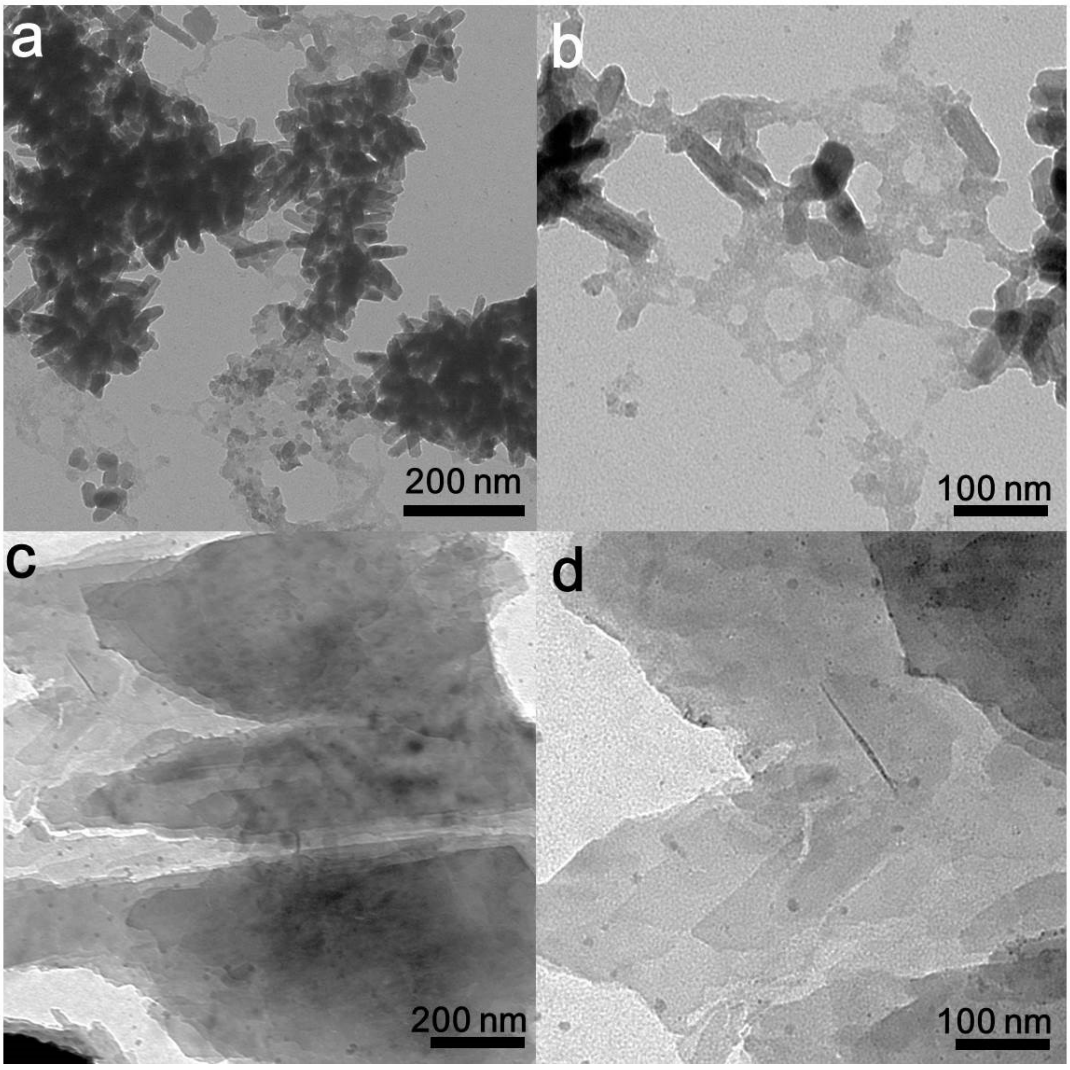

Fig.S6 Representative TEM images of the (a, b) Fe MOF and (c, d) Ni MOF.

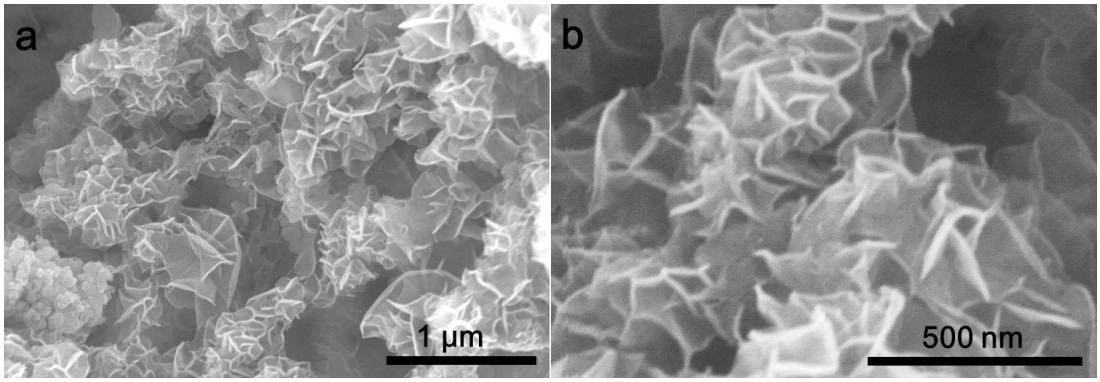

Fig.S7 Representative SEM images of the NiFe MOF.

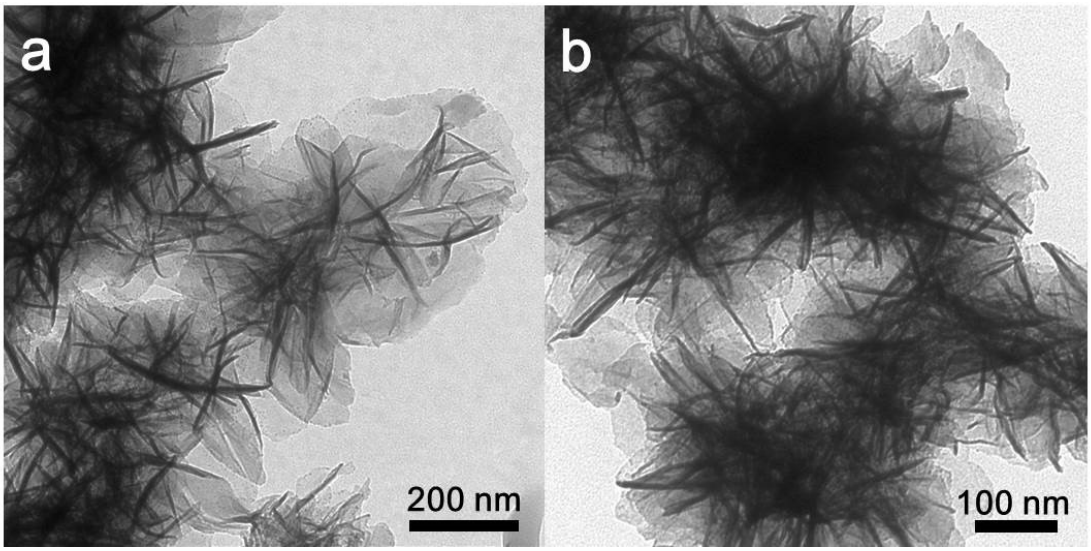

Fig.S8 Representative TEM images of the NiFe MOF.

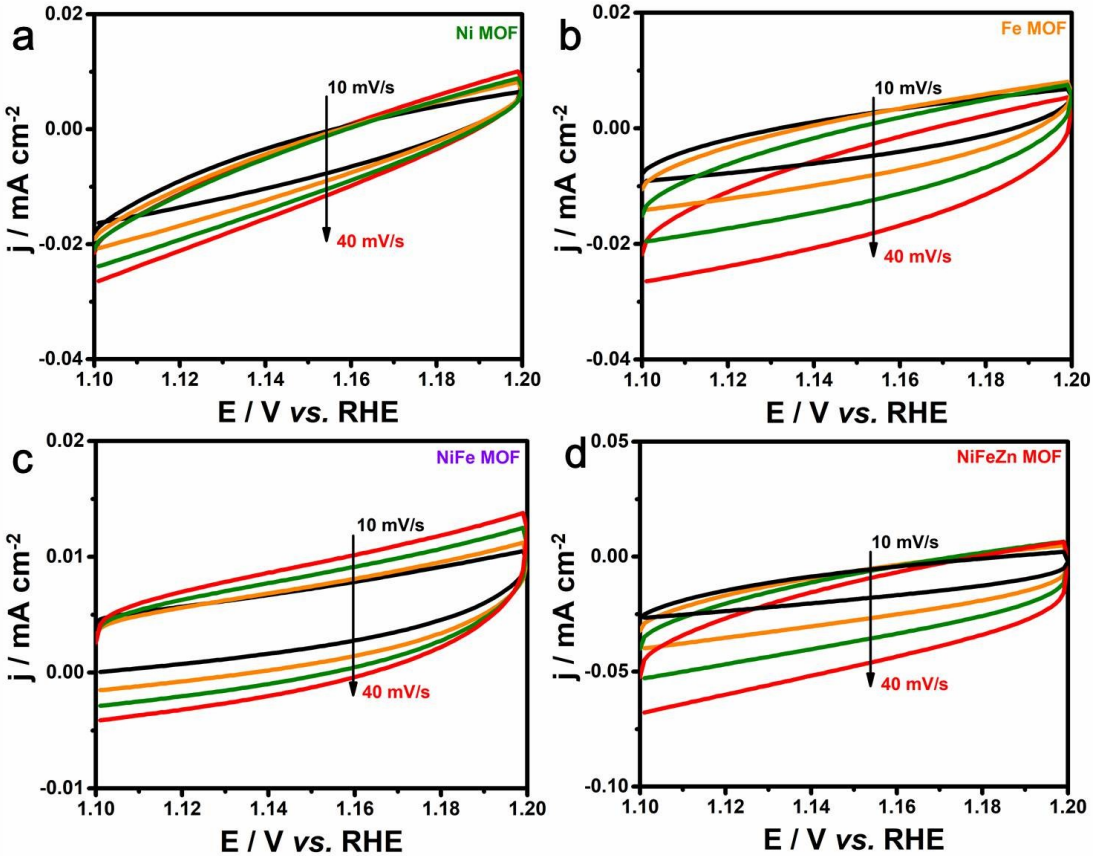

Fig.S9 CV curves of the (a) Ni MOF, (b) Fe MOF, (c) NiFe MOF, and (d) NiFeZn MOF with different scan rate.

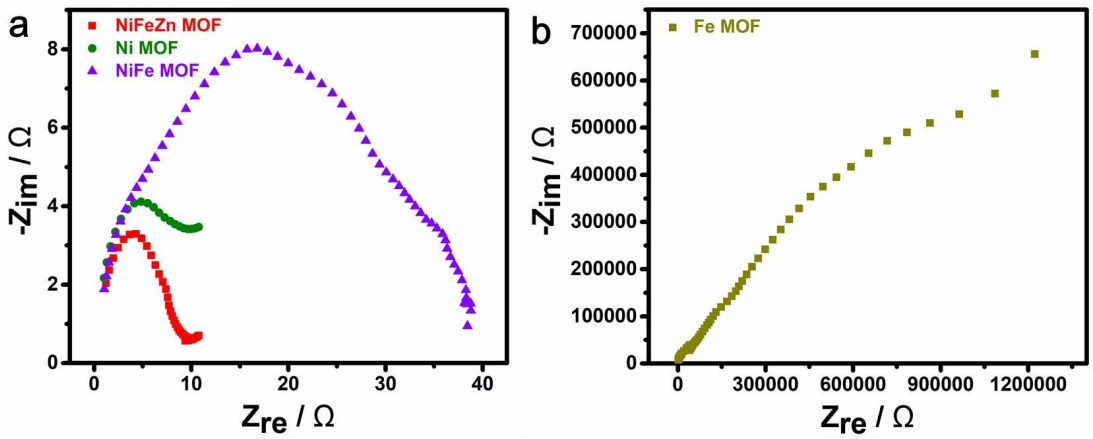

Fig.S10 Nyquist plots of the (a) Ni MOF, NiFe MOF, NiFeZn MOF, and (b) Fe MOF, at the potential of 1.6 V verus RHE.

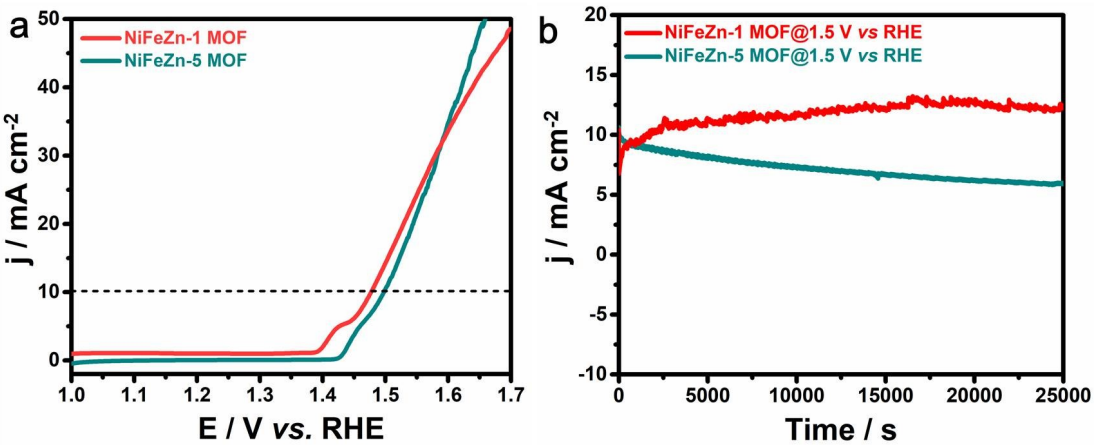

Fig.S11 (a) LSV curves of the NiFeZn-1 MOF and NiFeZn-5 MOF in 1 M KOH solution at the scan rate of 5 mV/s. (b) CA curves of the NiFeZn-1 MOF and NiFeZn-5 MOF at the potential of 1.5 V *vs* RHE.

Table S1 OER performance of different catalysts in alkaline water solution

Catalyst	ŋ@10 mA·cm^{-2}	Tafel slope (mV·dec^{-1})	Reference
NiFeZn MOF	233 mV	37.8	This work
CoNi MOF	276	55.6	[1]
NDA/MWCNTs-a	285	73	[2]
NiCo-MOF	310	106.3	[3]
Fe–Ni LDH/MOFs	255	24	[4]
CoO/CoP-NC	268	88	[5]
Mo-$(CoP_2)_{0.5}$-10	251	120.1	[6]
Co_2P@NPC	300	69.5	[7]
Fe-MIL-88B	310	/	[8]

References

1. X. Zhang, J. Luo, K. Wan, D. Plessers, B. Sels, J. Song, L. Chen, T. Zhang, P. Tang, J. R. Morante, J. Arbiol and J. Fransaer, *J. Mater. Chem. A*, 2019, **7**, 1616-1628.
2. S. Kiran, G. Yasmeen, Z. Shafiq, A. Abbas, S. Manzoor, D. Hussain, R. Adel Pashameah, E. Alzahrani, A. K. Alanazi and M. Naeem Ashiq, *Fuel*, 2023, **331**.
3. Q. Liu, J. Chen, P. Yang, F. Yu, Z. Liu and B. Peng, *Int. J. Hydrogen Energy*, 2021, **46**, 416-424.
4. J. Huo, Y. Wang, L. Yan, Y. Xue, S. Li, M. Hu, Y. Jiang and Q. G. Zhai, *Nanoscale*, 2020, **12**, 14514-14523.
5. K. Chen, Y. Cao, W. Wang, J. Diao, J. Park, V. Dao, G.-C. Kim, Y. Qu and I.-H. Lee, *J. Mater. Chem. A*, 2023, **11**, 3136-3147.
6. W. Peilin, L. Gao, L. Dong, Z. Lin and L. Cui, *Int. J. Hydrogen Energy*, 2023, **48**, 14543-14553.
7. P. Wei, X. Sun, Z. He, F. Cheng, J. Xu, Q. Li, Y. Ren, J. He, J. Han and Y. Huang, *Fuel*, 2023, **339**, 127303.
8. P. Zhao, X. Hua, W. Xu, W. Luo, S. Chen and G. Cheng, Catal. Sci. Technol., 2016, 6, 6365-6371